

**Homophily-Based Social Group Formation in a Spin Glass Self-Assembly Framework**Jan Korbelt<sup>1,2</sup>, Simon D. Lindner<sup>1,2</sup>, Tuan Minh Pham,<sup>1,2,3</sup> Rudolf Hanel,<sup>1,2</sup> and Stefan Thurner<sup>1,2,4,\*</sup><sup>1</sup>Section for the Science of Complex Systems, CeMSIIS, Medical University of Vienna, Spitalgasse 23, A-1090 Vienna, Austria<sup>2</sup>Complexity Science Hub Vienna, Josefstädterstrasse 39, A-1080 Vienna, Austria<sup>3</sup>Niels Bohr Institute, Blegdamsvej 17, 2100 Copenhagen, Denmark<sup>4</sup>Santa Fe Institute, 1399 Hyde Park Road, Santa Fe, New Mexico 87501, USA (Received 15 July 2022; revised 18 October 2022; accepted 30 November 2022; published 30 January 2023)

Homophily, the tendency of humans to attract each other when sharing similar features, traits, or opinions, has been identified as one of the main driving forces behind the formation of structured societies. Here we ask to what extent homophily can explain the formation of social groups, particularly their size distribution. We propose a spin-glass-inspired framework of self-assembly, where opinions are represented as multidimensional spins that dynamically self-assemble into groups; individuals within a group tend to share similar opinions (intragroup homophily), and opinions between individuals belonging to different groups tend to be different (intergroup heterophily). We compute the associated nontrivial phase diagram by solving a self-consistency equation for “magnetization” (combined average opinion). Below a critical temperature, there exist two stable phases: one ordered with nonzero magnetization and large clusters, the other disordered with zero magnetization and no clusters. The system exhibits a first-order transition to the disordered phase. We analytically derive the group-size distribution that successfully matches empirical group-size distributions from online communities.

DOI: [10.1103/PhysRevLett.130.057401](https://doi.org/10.1103/PhysRevLett.130.057401)

Structure-forming systems form an important class of complex systems [1]. They are ubiquitous in natural and social systems, ranging from atoms forming molecules, polymers, colloids, and micelles to people forming structured societies. The theory of *self-assembly* [2] describes the emergence of higher-order structures from elementary components. Applications include molecular self-assembly [3], lipid bilayers and vesicles [4], microtubules and molecular motors [5], Janus particles [6,7], other types of patchy particles [8], and RNA self-assembly [9]. The thermodynamics of self-assembled systems can be described sufficiently well with the grand-canonical ensemble for large systems. This is no longer true for small systems consisting of dozens or hundreds of particles. Correct results are obtained from the canonical ensemble with an appropriate correction to the entropic functional that correctly accounts for the statistics of structure formation [10].

Social group structures emerge from interactions between individuals. While traditional approaches explore social group formation under endogenous factors [11–13], more recent works attempt to explain its structures as a consequence of opinion formation [14–17]. Within this framework, groups are considered as clusters of homogeneous agents whose opinions evolve under the joint effects of *structural balance*, the tendency to resolve tension in unbalanced triadic interactions [18], and *homophily*, the preference of like-minded individuals to cluster [19,20]. Both approaches can explain the

fragmentation of society into well-connected groups of uniform opinions, sometimes referred to as *echo chambers* [21–26]. Spin glass Hamiltonians have been used on static social interaction networks to quantify the amount of social stress of the entire society [26], or that of each individual [27]. Social stress plays the role of energy and measures opinion similarity between individuals. Spin glass models were extensively studied on various network topologies, including fully connected [28–31], Barabási-Albert [32,33], small-world [34], more general [35], and coevolutionary, dynamic networks [36–38]; see Ref. [39] for a review. A similar idea of considering group formation as a way to maximize payoff through local homophilic interaction has led Javarone and Marinazzo [40] to the observation of a transition between the “group” and the “individual” phases upon varying the ratio between individual payoff and group payoff.

Obviously, the formation of friendship groups from individuals that randomly encounter each other cannot be realistically described on static networks. The theory of self-assembly offers an attractive alternative that could explain the endogenous emergence of social groups. To capture the interplay of opinion dynamics and group formation, the assumption of a stochastic rule for establishing social ties based on the similarity of opinions is reasonable.

To realize such a model, we assume an attractive interaction between individuals based on the proximity

of their opinions [27]. Opinions are represented by Ising-like spin vectors in  $G$  dimensions, each dimension corresponding to one binary opinion on a specific topic; the more aligned these vectors, the stronger the attractive force and the more likely they will form a friendly social tie. The main idea behind the model is that people tend to form friendship groups with like-minded individuals. They can also form hostile relations with individuals—typically from other groups. Entertaining a friendship relation with an individual with a drastically different opinion creates *social stress*. To reduce it, one can either change opinions or move to another group.

To overcome the main limitation of previous models—the predefined social network topology—we assume that individuals create the social network by dynamically interacting with each other and forming social links stochastically. We assume that every individual has a typical (average) number of positive connections within their group. At times, with a certain probability, people meet individuals from other groups. Links between individuals that belong to different groups are typically negative since they tend to have nonaligned opinion vectors. We assume that the probability of establishing a new (positive or negative) link between two individuals is proportional to the number of links both individuals have. The new link is positive if two individuals share more than half of their opinions; the link is negative if the majority of opinions are different. In the model, the social network emerges dynamically; only the local quantities such as each individual’s typical degree (the number of social interactions) are needed as an input. The resulting equilibrium group-size distribution can then be derived using the theory of self-assembly [10]. The distribution depends on the “temperature”  $T$ , which represents the willingness to change one’s opinion or to change the group. We study the phase structure (location of tipping points) of the model and compute the group-size distribution that is compared to real data. We confirm all analytical findings with straightforward Monte Carlo (MC) simulations. The core of the model is a social stress function (Hamiltonian) that every individual tries to minimize by changing either their opinion or their group membership.

*Self-assembly of spin glass.*—Let us consider  $n$  individuals with  $g$  binary opinions (spin vectors). We denote the  $j$ th opinion of individual  $i$  by  $s_i^j \in \{-1, 1\}$ . The spin vector of the  $i$ th individual is  $\mathbf{s}_i = \{s_i^1, \dots, s_i^g\}$ . We define the homophily between two individuals as the normalized dot product,  $\mathbf{s}_i \cdot \mathbf{s}_j = (1/g) \sum_{l=1}^g s_i^l s_j^l$ . Individuals can form clusters of any size,  $k \in \{1, \dots, n\}$ . We denote the number of groups of size  $k$  by  $n^{(k)}$ ; these fulfill  $\sum_{k=1}^n kn^{(k)} = n$ , where  $\cdot^{(k)}$  denotes the dependence of a quantity on a given group size  $k$ . A group of size  $k$  is given by  $\mathcal{G}^{(k)} = \{i_1, \dots, i_k\}$ . Following Ref. [27], we define the *group Hamiltonian* as

$$\begin{aligned}
 H(\mathbf{s}_{i_1}, \dots, \mathbf{s}_{i_k}) := & -\phi \frac{J}{2} \sum_{ij \in \mathcal{G}^{(k)}} A_{ij} \mathbf{s}_i \cdot \mathbf{s}_j \\
 & + (1 - \phi) \frac{J}{2} \sum_{i \in \mathcal{G}^{(k)}, j \notin \mathcal{G}^{(k)}} A_{ij} \mathbf{s}_i \cdot \mathbf{s}_j \\
 & - h^{(k)} \sum_{i \in \mathcal{G}^{(k)}} \mathbf{s}_i \cdot \mathbf{w},
 \end{aligned} \tag{1}$$

where  $J > 0$  is the coupling constant, and  $A_{ij}$  is the (dynamical) adjacency matrix of the underlying interaction network. The first term corresponds to homophilic intra-group interactions. The second term captures the intergroup interactions. The parameter  $\phi$  weights the relative importance of intragroup and intergroup stress. The last term corresponds to an external bias caused, e.g., by the mass media,  $h^{(k)}$  is the local external field that encodes the strength of that bias, and  $\mathbf{w}$  is a weight vector, measuring sensitivity to that bias. We take  $\mathbf{w} = \{1, \dots, 1\}$ . As discussed in Ref. [27], for  $G = 1$  the model reduces to the spin model of Mattis type [41] (also used in Refs. [42,43]). This model has no frustration on effective spins  $\tau_i = \epsilon_i s_i$ ,  $i \in \mathcal{G}$ , where  $\epsilon_i \epsilon_j = 1$  for  $j \in \mathcal{G}$  and  $\epsilon_i \epsilon_j = -1$  if  $j \notin \mathcal{G}$ . Thus, the effective Hamiltonian in terms of  $\tau_i$  is the usual Ising Hamiltonian with no negative interactions. This is, however, not possible for  $G > 1$ , and therefore we inevitably end with frustrated interactions (at least for some opinions).

The relative number of clusters of size  $k$  is  $\wp^{(k)} = n^{(k)}/n$ . The equilibrium group-size distribution can be expressed as [10]

$$\wp^{(k)} = \Lambda^k \mathcal{Z}^{(k)}, \tag{2}$$

where  $\mathcal{Z}^{(k)} = (n^{k-1}/k!) \sum_{\mathbf{s}_{i_1}, \dots, \mathbf{s}_{i_k}} e^{-\beta H(\mathbf{s}_{i_1}, \dots, \mathbf{s}_{i_k})}$  is the partition function of a group with size  $k$ ,  $\beta = (1/k_B T)$  is the inverse temperature (using  $k_B = 1$ ), and  $\Lambda$  is the normalization obtained from  $\sum_{k=1}^n k \wp^{(k)} = \sum_{k=1}^n k \Lambda^k \mathcal{Z}^{(k)} = 1$ , which is a polynomial equation in  $\Lambda$  of order  $n$ . The number of groups per individual is  $M = \sum_{k=1}^n n^{(k)}/n = \sum_{k=1}^n \wp^{(k)}$  and the average group size is  $C = \sum_{k=1}^n kn^{(k)}/\sum_{k=1}^n n^{(k)} = 1/M$ . The average opinion vector of group  $\mathcal{G}^k$  is defined as  $\mathbf{m}^{(k)} = \sum_{i \in \mathcal{G}^{(k)}} \mathbf{s}_i$ . The average weighted opinion  $m^{(k)} = \mathbf{m}^{(k)} \cdot \mathbf{w}$  can be expressed as  $m^{(k)} = -(1/\beta)(\partial \log \mathcal{Z}^{(k)}/\partial h^{(k)})$ ; the total magnetization divided by the number of individuals is therefore  $m = \sum_k \wp^{(k)} m^{(k)}$ .

*Simulated annealing.*—To overcome the main limitation of previous models, i.e., the full specification of the adjacency interaction matrix, we follow the approach used in statistical physics of spin systems called *simulated annealing* or *configuration model* [32]. We approximate  $A_{ij} \approx (q_i^{(k)} q_j^{(k)})/2C^{(k)}$ , if  $i$  and  $j \in \mathcal{G}^{(k)}$ . Here  $q_i^{(k)}$  is the intragroup degree of node  $i$  and  $C^{(k)}$  is the total number of intragroup links in a group of size  $k$ . Similarly,

$A_{ij} \approx (q_i^{(k,l)} q_j^{(l,k)} / 2C^{(k,l)})$  for  $i \in \mathcal{G}^{(k)}$  and  $j \notin \mathcal{G}^{(k)}$ . Here  $q_i^{(k,l)}$  is the intergroup degree of node  $i$  to all other groups of size  $l$  and  $C^{(k,l)}$  is the total number of interlinks between groups of size  $k$  and  $l$ . The simulated annealing approach can be understood as a dynamical friendship network formation framework based on the individuals' opinions and their desired number of friendship links.

**Mean-field approximation.**—Assuming the validity of a mean-field approach, the group Hamiltonian can be approximated by  $H_{\text{MF}}^{(k)}(\mathbf{s}_{i_1}, \dots, \mathbf{s}_{i_k}) = \sum_{i \in \mathcal{G}^{(k)}} \mathbf{s}_i \cdot \mathbf{H}_i^{(k)}$ , where

$$\mathbf{H}_i^{(k)} = -\frac{\phi J}{2} q_i^{(k)} \mathbf{m}^{(k)} + \frac{(1-\phi)J}{2} \sum_l q_i^{(k,l)} \mathbf{m}^{(l)} - h^{(k)}. \quad (3)$$

We define  $H_i^{(k)} = \mathbf{H}_i^{(k)} \cdot \mathbf{w}$ . By calculating the mean-field partition function and taking the derivative with respect to the external field, we get that the average group opinion  $m^{(k)}$  can be expressed as

$$m^{(k)} = \sum_{i \in \mathcal{G}^{(k)}} \tanh[\beta H_i^{(k)}(m^{(l)})]. \quad (4)$$

A detailed derivation is found in the Supplemental Material (SM) [44]. Let us now consider that the intragroup and intergroup degree distributions,  $q^{(k)}$  and  $q^{(k,l)}$ , are random variables with distributions  $p(q^{(k)})$  and  $\mathfrak{p}(q^{(k)})$ , respectively. Then we can formulate the set of self-consistency equations,

$$m^{(k)} = k \sum_{q^{(k)}, q^{(k,l)}} p(q^{(k)}) p(q^{(k,l)}) \tanh(\beta H^{(k)}), \quad (5)$$

where  $H^{(k)}$  depends on  $q^{(k)}$ ,  $q^{(k,l)}$ , and  $m^{(l)}$ . Thus, we obtain a system of  $n$  coupled equations for  $m^{(k)}$ .

**Self-consistency equation with no intergroup interactions.**—The set of self-consistency equations simplifies dramatically for the case  $\phi = 1$ , where no intergroup interactions exist. The equations decouple, and we obtain one self-consistency equation for every  $m^{(k)}$ . We first focus on the simple case of the fully connected intergroup network, where  $p(q^{(k)}) = \delta(q^{(k)}, k-1)$ . In this case, the numerical value of the average magnetization per person is depicted in Fig. 1. We observe the first-order phase transition between disordered phase and the coexistence phase, where both disordered and ordered phase exists. These phases are separated by the *binodal* temperature  $T_B$ , which describes the point when the system, originally in the ordered phase, starts to disorder when increasing the temperature. Note that the *spinodal* temperature  $T_S$  tends to zero. The spinodal temperature describes the point where the particles spontaneously start forming large groups when starting in the disordered phase and decreasing the

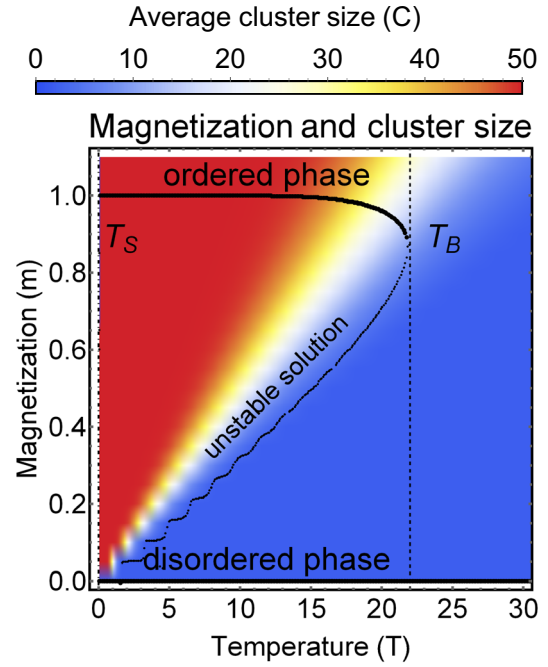


FIG. 1. Total magnetization  $m$  as a function of the temperature  $T$  for  $n = 50$ ,  $G = 3$ , and  $J = 1$ , without external field. The heat map shows the average cluster size  $C$  as a function of  $m$  and  $T$ . We observe the presence of a critical temperature  $T_B$  above which the self-consistency equations yield a single solution,  $m = 0$ . Below this temperature, we observe two stable solutions, a coexistence of a disordered phase, characterized by the absence of large clusters (average cluster size is 1), and an ordered phase that is characterized by the existence of one large cluster with all particles having the same opinion vector. By increasing the temperature to the critical temperature, the cluster starts to disintegrate rapidly while the magnetization remains relatively stable.

temperature. All individuals are free with random opinion in the disordered phase. In the ordered phase, all individuals form a single cluster with the same opinion. The existence of the first-order transition between the ordered and a group phase has been suggested in Ref. [40].

The average cluster size rapidly decreases near the binodal temperature while the overall magnetization remains relatively stable. However, at the critical temperature, the magnetization is still significantly nonzero. At the same time, the average cluster size decreases continuously toward one. The dependence of the phase diagram on the external field and minimum cluster size is shown in SM [44].

**Monte Carlo simulations.**—We perform the Monte Carlo simulations to confirm the phase diagram obtained from solving the self-consistency equations for the magnetization numerically. We use the standard Metropolis algorithm for  $n = 50$  individuals and three opinions,  $G = 3$ . Each MC step consists of  $n$  spin updates (flips) of one spin element chosen randomly, followed by randomly choosing one individual and moving them from the current group to

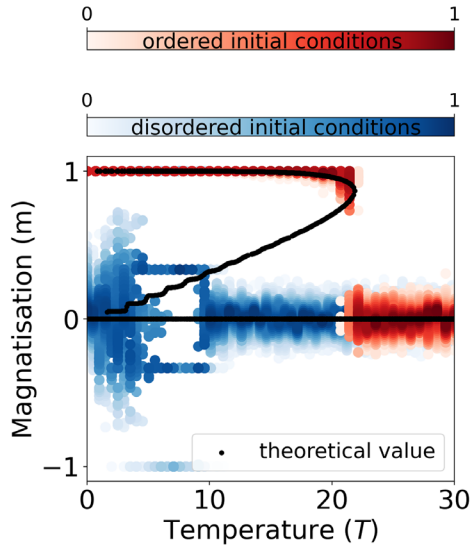


FIG. 2. Magnetization as obtained from Monte Carlo simulations for the same parameters as in Fig. 1. For each temperature, 100 independent runs with  $5 \times 10^4$  steps were performed. We started from two types of initial conditions—one in the ordered phase, where all individuals are in one large group with identical initial opinions (red), and from the disordered phase, where all individuals form a separate group with a random initial opinion (blue). For each temperature, the histogram of magnetization was established. The darker the color, the larger the frequency; see color bars. The black curve shows the theoretical magnetization obtained from the self-consistency equations. For the ordered phase, we observe the perfect agreement with the theory, and the critical temperature corresponds with the predicted one. For the disordered phase, we see that the average temperature also corresponds to the predicted value,  $m = 0$ . However, the fluctuations are larger.

another group—or by creating a new group consisting of only that individual. If the individual is already solitary, it has to attach to one of the existing groups. The MC temperature for opinion flips and group changes are the same, i.e., both spin flips and group changes are accepted with probability  $\min\{1, \exp(-\beta\Delta H_{\text{tot}})\}$ , where  $H_{\text{tot}} = \sum_{\mathcal{G}^{(k)}} H(\mathcal{G}^{(k)})$  is the sum over all group Hamiltonians. For each temperature, we perform 100 independent simulations with  $5 \times 10^4$  MC steps. We repeat the simulation for two initial conditions corresponding to the two equilibrium phases: one in the ordered and one in the disordered phase. For ordered initial condition, we observe that the particles stay in one cluster below critical temperature (Fig. 2 in red). For the initial condition in the disordered phase, the magnetization clearly fluctuates around zero (Fig. 2 in blue). For lower temperatures, the system can get stuck in a local minimum, seen by the fact that the magnetization fluctuates more and we observe a “quantization” effect. Even for very low temperatures, large groups are rare to form and, therefore,  $T_S$  is close to zero. In SM [44], we investigate the dependence of the

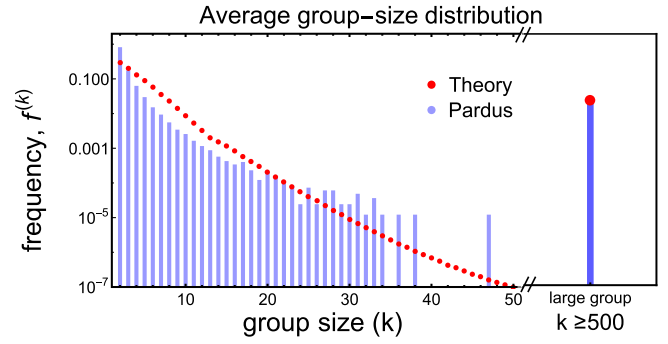


FIG. 3. Semi-logarithmic frequency distribution of group sizes obtained from the Pardus dataset (blue, from Ref. [14]) and the prediction of the self-assembly group-formation model (red). The group-size distribution is shown for group sizes between 2 and 50. For large groups of more than 500 players, the probabilities of observing a group with an exact particular size are very small. Thus we aggregate the probabilities for observing a group larger than 500 into one single bin. For both small and large groups, the theoretical prediction fits the group-size distribution of Pardus dataset well.

phase diagram on the minimum group size, external field, and initial conditions.

*Group-size distribution of Pardus network.*—Finally, we compute the emerging group-size distribution from the presented approach and compare it with a real dataset of an open-ended massive multiplayer online game called Pardus [47]. Players in Pardus form friendships and enmity relations based on economic (in the virtual world) and social activities. We focus on only one type of social interaction, the players’ communication. The dataset consists of 1239 days, each day with about 1000–1600 active players (players with at least one communication event with another player). We adopt a picture where a communication event between players creates a link between them. Each connected component in this communication network corresponds to one group. Typically, we observe one giant connected component with several hundreds of participants and many small groups with sizes ranging from 2 to 50. A typical communication network on one day is shown in the SM [44]. The average group-size distribution is obtained by averaging group-size distributions over all days. We compare the so-obtained group-size distribution of the friendship network with the theoretical prediction from the self-assembly model in Fig. 3. The intragroup degree distribution, obtained from Ref. [14], can be well approximated with a truncated geometric distribution,  $p_a^{(k)}(q^{(k)}) = a(1-a)^{q^{(k)}-1}/[1-(1-a)^k]$ , where  $q^{(k)} \in \{1, \dots, k-1\}$ . with  $a = 0.6$ , as shown in SM. For clarity, we show the frequency of observing a group of size  $k$ ,  $f^{(k)} = n^{(k)}/M = n/M \cdot \varphi^{(k)}$ . By fitting the temperature, we obtain the theoretical group-size distribution, which corresponds to the real group-size distribution of the Pardus dataset. Because of the varying number of players across days, we

fit the group-size distribution for small groups in the range between 2 and 50 and aggregate the probability of observing one large group of more than 500 (giant component). Medium-size groups (51–499 players) do not appear in the dataset. It is obvious that the theoretical group-size distribution explains the empirical Pardus data well. Interestingly, the Gini coefficient, which quantifies statistical dispersion, for both the empirical distribution ( $G = 0.900$ ) and the theoretical model ( $G = 0.901$ ), is close to the transition point of  $G = 0.86$  observed in several studies on percolation cluster size distribution (see Ref. [48] for a recent review).

*Discussion.*—The presented self-assembly model for social group formation offers a new view on coevolving dynamics of group and opinion formation. The framework of spin glass self-assembly is purely based on local information, i.e., local social stress and the number of contacts (degrees) of individuals. Our main result is to show the existence of a critical temperature (binodal temperature) above which large groups disintegrate and that the opposite process, i.e., spontaneous group formation by lowering the temperature, is not possible when the external field is zero. We confirm these theoretical predictions with Monte Carlo simulations.

We are able to make a further testable prediction concerning the emerging group sizes in the model society. To compare with real data, we used the social network of the Pardus computer game, for which we have exact knowledge of group formation and sizes. Using the actual degree distribution of the friendship networks as inferred from the dataset as an input to our model, we are able to compute a group-size distribution that corresponds almost perfectly with the empirical group-size distribution in the Pardus data. Compared with recent work [40], our study was able to take into account aspects such as social network topology, local homophily effects (not only the global average opinion), and coevolution of opinions and the friendship links. Therefore, as a result, we obtained a complex phase diagram, including the previously observed first-order transition between individual and group phases and other phenomena, such as bifurcation of the average cluster size, or dependence on the external field.

The model has a few limitations. The most important is that higher-order motives, such as those known from social balance, are not recovered correctly. In many social networks, some of the higher-order motifs are over- or underrepresented, compared to configuration model approach. To get these statistics right, more advanced approaches known from spin glasses, such as the Bethe approach [49], belief propagation [50], the cavity method [51], or other generalizations of the configuration model, could be useful. A second limitation is a correlation between different opinions and the fact that this correlation can change over time. In reality, people define their *belief system* where the opinions are correlated [52,53], and the

correlations can evolve in time. Finally, the presented framework operates on a single network where links between individuals influence all opinions of their friends or enemies. For more realism, one would need to consider a multilayer network that represents different environments (family, work, leisure time, social networks, etc.) with links of different types where each layer can influence only certain types of opinions.

We thank Michael Szell and Peter Klimek for providing and assisting us with the Pardus data. The project was supported by the Austrian Science Fund (FWF) Project No. P 34994 and Project No. P 33751 and Austrian Science Promotion Agency (FFG) Project Grant No. 857136.

---

\* stefan.turner@meduniwien.ac.at

- [1] S. Thurner, R. Hanel, and P. Klimek, *Introduction to the Theory of Complex Systems* (Oxford University Press, New York, 2018).
- [2] G. M. Whitesides and B. Grzybowski, *Science* **295**, 2418 (2002).
- [3] G. M. Whitesides, J. P. Mathias, and C. T. Seto, *Science* **254**, 1312 (1991).
- [4] J. N. Israelachvili, D. J. Mitchell, and B. W. Ninham, *Biochim. Biophys. Acta* **470**, 185 (1977).
- [5] I. S. Aranson and L. S. Tsimring, *Phys. Rev. E* **74**, 031915 (2006).
- [6] R. Fantoni, A. Giacometti, F. Sciortino, and G. Pastore, *Soft Matter* **7**, 2419 (2011).
- [7] A. Walther and A. H. Müller, *Chem. Rev.* **113**, 5194 (2013).
- [8] N. Kern and D. Frenkel, *J. Chem. Phys.* **118**, 9882 (2003).
- [9] W. W. Grabow and L. Jaeger, *Acc. Chem. Res.* **47**, 1871 (2014).
- [10] J. Korbelt, S. D. Lindner, R. Hanel, and S. Thurner, *Nat. Commun.* **12**, 1127 (2021).
- [11] M. Hechter, *Am. J. Sociol.* **84**, 293 (1978).
- [12] S. Gueron and S. A. Levin, *Math. Biosci.* **128**, 243 (1995).
- [13] E. P. Zeggelink, F. N. Stokman, and G. G. Van De Bunt, *J. Math. Sociol.* **21**, 29 (1996).
- [14] P. Klimek, M. Diakonova, V. M. Eguíluz, M. San Miguel, and S. Thurner, *New J. Phys.* **18**, 083045 (2016).
- [15] C. Zingg, G. Casiraghi, G. Vaccario, and F. Schweitzer, *Entropy* **21**, 901 (2019).
- [16] S. Schweighofer, D. Garcia, and F. Schweitzer, *Chaos* **30**, 093139 (2020).
- [17] F. Schweitzer and G. Andres, *Phys. Rev. E* **105**, 044301 (2022).
- [18] F. Heider, *J. Psychol.* **21**, 107 (1946).
- [19] M. McPherson, L. Smith-Lovin, and J. M. Cook, *Annu. Rev. Sociol.* **27**, 415 (2001).
- [20] G. A. Huber and N. Malhotra, *J. Polit.* **79**, 269 (2017).
- [21] S. A. Marvel, S. H. Strogatz, and J. M. Kleinberg, *Phys. Rev. Lett.* **103**, 198701 (2009).
- [22] S. Currarini, J. Matheson, and F. Vega-Redondo, *Eur. Econ. Rev.* **90**, 18 (2016).
- [23] A. M. Belaza, K. Hoefman, J. Ryckebusch, A. Bramson, M. Van Den Heuvel, and K. Schoors, *PLoS One* **12**, e0183696 (2017).

- [24] P. J. Górski, K. Bochenina, J. A. Hołyst, and R. M. D'Souza, *Phys. Rev. Lett.* **125**, 078302 (2020).
- [25] T. Minh Pham, I. Kondor, R. Hanel, and S. Thurner, *J. R. Soc. Interface* **17**, 20200752 (2020).
- [26] T. Minh Pham, A. C. Alexander, J. Korbelt, R. Hanel, and S. Thurner, *Sci. Rep.* **11**, 17188 (2021).
- [27] T. M. Pham, J. Korbelt, R. Hanel, and S. Thurner, *Proc. Natl. Acad. Sci. U.S.A.* **119**, e2121103119 (2022).
- [28] R. B. Griffiths, C.-Y. Weng, and J. S. Langer, *Phys. Rev.* **149**, 301 (1966).
- [29] S. Galam, *Physica (Amsterdam)* **230A**, 174 (1996).
- [30] M. Kochmański, T. Paszkiewicz, and S. Wolski, *Eur. J. Phys.* **34**, 1555 (2013).
- [31] L. Colonna-Romano, H. Gould, and W. Klein, *Phys. Rev. E* **90**, 042111 (2014).
- [32] G. Bianconi, *Phys. Lett. A* **303**, 166 (2002).
- [33] C. Merger, T. Reinartz, S. Wessel, C. Honerkamp, A. Schuppert, and M. Helias, *Phys. Rev. Res.* **3**, 033272 (2021).
- [34] A. Pękalski, *Phys. Rev. E* **64**, 057104 (2001).
- [35] S. N. Dorogovtsev, A. V. Goltsev, and J. F. F. Mendes, *Phys. Rev. E* **66**, 016104 (2002).
- [36] C. Biely, R. Hanel, and S. Thurner, *Eur. Phys. J. B* **67**, 285 (2009).
- [37] D. Sornette, *Rep. Prog. Phys.* **77**, 062001 (2014).
- [38] T. Raducha, M. Wilinski, T. Gubiec, and H. E. Stanley, *Phys. Rev. E* **98**, 030301 (2018).
- [39] S. N. Dorogovtsev, A. V. Goltsev, and J. F. Mendes, *Rev. Mod. Phys.* **80**, 1275 (2008).
- [40] M. A. Javarone and D. Marinazzo, *PLoS One* **12**, e0187960 (2017).
- [41] D. Mattis, *Phys. Lett.* **56A**, 421 (1976).
- [42] G. Facchetti, G. Iacono, and C. Altafini, *Proc. Natl. Acad. Sci. U.S.A.* **108**, 20953 (2011).
- [43] R. Singh, S. Dasgupta, and S. Sinha, *Europhys. Lett.* **105**, 10003 (2014).
- [44] See Supplemental Material at <http://link.aps.org/supplemental/10.1103/PhysRevLett.130.057401> for more details, which includes [45,46].
- [45] C. Kuehn and C. Bick, *Sci. Adv.* **7**, eabe3824 (2021).
- [46] H. Zhu, S. Dong, and J.-M. Liu, *Phys. Rev. B* **70**, 132403 (2004).
- [47] M. Szell, R. Lambiotte, and S. Thurner, *Proc. Natl. Acad. Sci. U.S.A.* **107**, 13636 (2010).
- [48] A. Ghosh, S. Biswas, and B. K. Chakrabarti, *Front. Phys.* **10**, 990278 (2022).
- [49] H. A. Bethe, *Proc. R. Soc. A* **150**, 552 (1935).
- [50] S. Yoon, A. V. Goltsev, S. N. Dorogovtsev, and J. Mendes, *Phys. Rev. E* **84**, 041144 (2011).
- [51] M. Mézard and G. Parisi, *J. Stat. Phys.* **111**, 1 (2003).
- [52] N. Rodriguez, J. Bollen, and Y.-Y. Ahn, *PLoS One* **11**, 1 (2016).
- [53] N. E. Friedkin, A. V. Proskurnikov, R. Tempo, and S. E. Parsegov, *Science* **354**, 321 (2016).